Optimal thermal energy management of a distributed energy system formed by a solar membrane distillation plant and a greenhouse

Juan D. Gil[a], J.D. Álvarez[a,*], Lidia Roca[a,b], J.A. Sánchez-Molina[a], Manuel Berenguel[a], F. Rodríguez[a]

[a] *Centro Mixto CIESOL, ceiA3, Universidad de Almería. Ctra. Sacramento s/n, Almería 04120, Spain; {juandiego.gil,jhervas,jorgesanchez,beren,frrodrig}@ual.es*
[b] *CIEMAT-Plataforma Solar de Almería, Ctra. de Senés s/n, Tabernas 04200, Almería, Spain; lidia.roca@psa.es*

Abstract

The scarcity of water in Mediterranean countries in general and in Almería (Southeast Spain) in particular could compromise one of its main economic drivers; agriculture. One of the possible solutions consists on the combination of thermal desalination technologies with greenhouse crop production. In this sense, Membrane Distillation (MD) becomes an attractive technology since it can be easily combined with solar energy, thus forming sustainable and efficient plants. However, the combination of MD processes with greenhouses requires adequate control systems able to manage the operation of the facility. In this paper, a Distributed Model Predictive Controller (DMPC) is proposed for the efficient operation of a distributed energy system composed by a Solar Membrane Distillation (SMD) facility and a greenhouse. The controller is in charge of calculating the optimal feed flow rates for each of the MD modules included in the facility, according to the water requirements and the thermal efficiency of the SMD plant, one of the main weak points of the technology. Simulation results are presented showing how the DMPC approach converges to results similar to those of an optimal centralized formulation. However, when considering plants of industrial size, only the DMPC approach can be used due to

*Corresponding author.
Email address: jhervas@ual.es (J.D. Álvarez)

the high computational time required by the centralized controller. Finally, the automatic operation is compared with a manual one (non optimal one), showing that the thermal efficiency of the operation can be improved by 5 %, whereas the water demand is satisfied. This means important savings at industrial scale.
Keywords: Process control, Distributed control, Model Predictive control, Solar energy, Thermal efficiency, Agriculture.

1. Introduction

Almería is located in the Southeast Spain, in a semi-desertic zone with a severe problem of water scarcity. Nevertheless, agriculture is one of the economic drivers of this dry region, with more than 31034 greenhouse ha [1] thanks to the availability of untapped water resources, rivers or aquifers and the use of drip irrigation and efficient control systems, combined with its high agricultural potential due to the good climate conditions.

The development of a water-intensive agriculture has led this region to be highly competitive in international markets, but also the intensification of irrigation, and the required infrastructures (reservoirs, dams, canals, wells, pools) have ecological and social impacts which, in some cases, are already irreversible [2]. The development of irrigation in the Southeast of Spain is associated with the overexploitation of aquifers of major rivers, which urgently demands solutions to overcome this problem and make this economy sustainable regarding the use of water. As pointed out by [1], the horticultural sector is in the right path towards a green economy and the desalination and reclaimed water should be used for irrigation demand [3]. In fact, Spain is the leader in the use of distillate water for agriculture purposes [4], but two main drawbacks must be faced; the increment of salinity and boron in the soil [5], and the associated costs [6]. This is the reason why, reverse osmosis (RO) is the usual technology and the most commercially extended [7]. In spite of that, membrane distillation (MD) is a technology with potential which is gaining interest year after year [8]. Its principal advantages are: it requires low-grade thermal energy so that it can be

easily coupled with solar thermal systems [9], low electric power consumption, does not usually require chemical pretreatment, the quality of the product is excellent and insensitive to feed-water salinity, feed flow rate and temperature, which makes it suitable for zero-liquid discharge schemes. Due to this last advantage, MD can be used not only for desalting seawater, but also to produce clean water from contaminated feedwater [10], thus being useful to improve the quality of treated water for irrigation.

Although MD processes coupled with solar systems (SMD) are today relatively expensive compared to other desalination technologies [8], they could be a feasible solution for small applications in those places with high solar irradiance and water scarcity. Moreover, due to the low operating temperature, their operation and maintenance is simple and they can be easily coupled to small production plants.

Towards sustainable irrigated crops, a solar distillation system, such as an SMD, should be combined with an automatic control system. From the water control point of view in greenhouses, there are two research lines that can be combined: i) irrigation control techniques [11, 12, 13, 14] and ii) control strategies for the operation of the water generation source [15, 16]. If we consider a water storage system for irrigation, the first research line covers from the storage to the crop, while the second one deals with the control strategy from the water generation system to the storage. As pointed out by [11], in order to make the irrigation control strategies available for commercial purposes, the advantages of applying these strategies should be deeply analyzed. For example, in [14] a model predictive controller (MPC) with an event-based controller is proposed to maintain the soil humidity level, showing that it is possible to reduce 20 % the use of water in comparison to typical on/off controllers. On the other hand, if an adequate controller is applied to the water generation system, such as the one proposed in [16], in which an MPC is applied to an SMD facility, the costs of the water produced (and related to the use of the pumping system) can be reduced up to 10%.

Following the research line of advanced control strategies for the water gener-

ation source such as the one described in [15], this paper proposes a Distributed MPC (DMPC) strategy to operate an SMD system and produce water for a greenhouse. A controller based on an MPC technique [17] calculates the control law based on an objective function and a prediction model. In this case, the DMPC includes prediction models of the energy source (a heat generation system based on a solar field), the production system (membrane distillation units) and the consumption system (a greenhouse). Unlike [15], the objective function includes not only the volume of distillate but also a thermal energy index which is one of the main drawbacks of the MD technology. In addition, the proposed distillate generation system is a combination of different membrane technologies, which adds complexity to the problem.

In the proposed decentralized scheme [18] each agent solves an MPC problem and exchanges information with other agents. With the application of this technique the risk of failure is reduced because the system does not depend on one centralized control. Moreover, the communications between the agents and the centralized controller as well as and the computational power of a centralized approach are simplified, what could be essential in industrial plants in which the number of agents involved in the problem is greater.

DMPC techniques have been previously applied in multi-agent systems, specially in distributed energy systems [19, 20]. In particular, in the agricultural field, these kind of controllers have been applied to control irrigation canals [21, 22, 23]. The goal in these cases was to maintain the desired water levels in the different irrigation pools by acting over the canal gates. Since the dynamic of the water level in a pool depends on the evolution of the other pools located over long distances, the collaborative management included in the DMPC makes this technique suitable for an optimal operation of irrigation canals. In the present work the DMPC technique is used to manage the operation of the MD modules which act as agents of the distributed scheme. In this way, following the ideas presented in [24, 25], optimal feed flow rates are calculated in each agent to reduce the specific thermal energy and maintain the desired level of water for irrigation purposes. Simulation results with the DMPC are presented focused

on the case in which the available resources (i.e. feed water flow) are limited. Notice that in the MD modules employed in this work the maximum thermal efficiency is achieved when they work at minimum feed flow rate, whereas the maximum distillate production is achieved at maximum feed flow rate [26, 27]. Therefore, in the design phase, a tradeoff solution between the cost associated to pump the feed water (to increase the distillate production) and the thermal efficiency should be considered. In these specific cases, the use of a suitable controller could be very relevant for the successful implementation of these kind of facilities.

The paper is organized as follows. In Section 2, the case of study is presented. The models are described in Section 3. The centralized and distributed control algorithms are explained in Section 4. The performance of the controllers are depicted and analyzed in Section 5. Finally, conclusions are summarized in Section 6.

2. Case of study

The facility studied in this work basically consists on a distributed energy system composed by an SMD plant and a greenhouse (see Fig. 1). In this plant, the greenhouse acts as consumer, demanding fresh water for the irrigation of the crop, while the desalination plant acts as producer, providing the required fresh water. In addition, a storage tank (3 m^3) is used to connect both facilities. It should be remarked that the considered plant is a simulation use case based on the two real facilities presented in the following subsections.

2.1. Solar distillation plant

The SMD plant (see Fig. 2) is located at Plataforma Solar de Almería (PSA, www.psa.es, Southeast Spain), and it is one of the few MD plants totally described in the literature [28]. In this facility, the thermal energy required for the distillation process is provided by a solar field composed of flat-plate collectors. This solar field is directly connected to a storage tank (1,5 m^3) that is used as

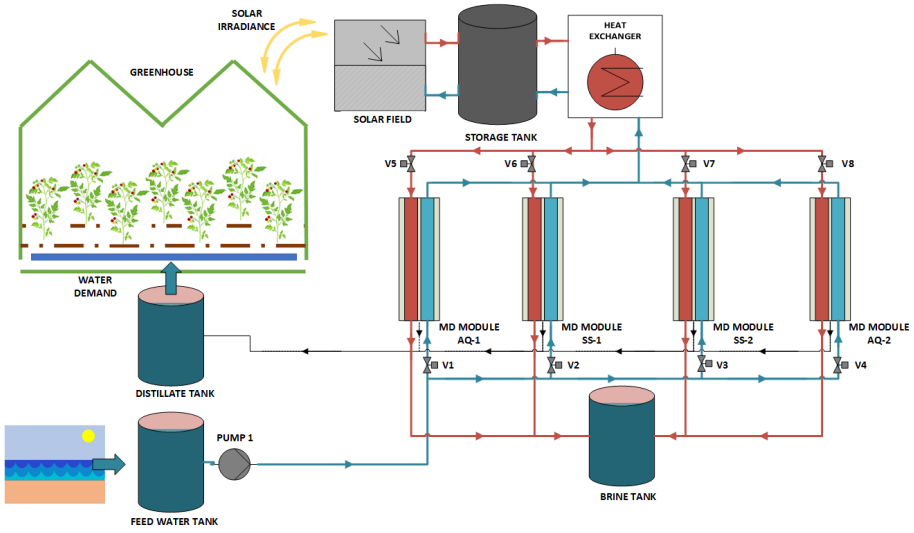

Figure 1: Schematic diagram of the facility simulated as case of study.

Figure 2: SMD pilot plant at PSA. From top to bottom and from left to right: solar field, Solar Spring module, and Aquastill module.

energy buffer system. Finally, the distillation module is coupled with the heat generation circuit through a heat exchanger.

There are several commercial MD modules available at PSA, which are based on different MD configurations. The two modules used in this work (see Fig. 2) are the Aquastill unit, which is based on the air-gap Membrane Distillation technology [27], and the Solar Spring one, which has a permeate-gap Membrane Distillation configuration [26]. Notice that in the case of study (see Fig. 1) four MD units (two of each commercial module) have been considered, in order to scale the distillate production of the desalination plant to the water requirements of a greenhouse.

Inside the MD unit (see Fig. 3) the sea water is firstly pumped trough the condenser channel of the module. Notice that, due to module design constraints, the feed flow rate has a limited operating range between 400 and 600 L/h. Afterwards, the feed fluid passes trough the heat exchanger, where it is heated with the recirculating fluid coming from the solar field, and then, it is circulated into the evaporator channel of the module. The evaporator inlet temperature varies between 60 and 80 °C, the upper limit is imposed by membrane materials, and the lower one is established because working at lower temperatures, the module produces very little distillate. The temperature difference created at both sides of the channels, produces a pressure difference that makes that the vapour molecules travel from the evaporator channel to the condenser one. At last, in the evaporator channel, the volatile components of the heated solution pass through a hydrophobic and micro-porous membrane (becoming distillate after a condensation process), whereas non volatile molecules are rejected in the form of brine.

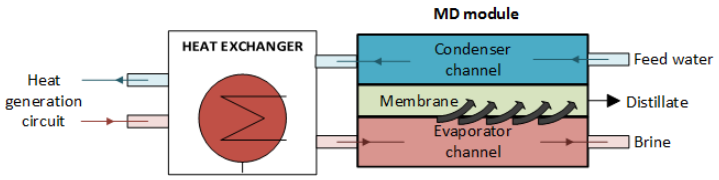

Figure 3: Schematic diagram of a single MD unit.

2.2. Greenhouse

The greenhouse (see Fig. 4) employed as reference in this work is located at the Experimental Station of Cajamar Foundation, situated also in the Southeast of Spain (40 km far from the PSA). This environment is composed by a multi-spam "Almeria-type" greenhouse (orientation E-W), with a surface of 821 m^2 and an area of cultivation of 616 m^2. The greenhouse has a cover of polyethylene equipped with an automatic ventilation system with side windows on the walls north and south, heating system fueled by biomass, diesel aerothermal system, LEDs lights, humidification and dehumidification system by condensation with a water extraction capacity of 900 L/day.

Figure 4: Greenhouse facilities. From left to right and from top to bottom: greenhouse, dropper and tomato crop lines.

The crop grows in rows with orientation N-S, inside coconut coir bags, with three droppers and six plants each. Throughout the crop season, several internal and external measurements were continuously monitored. Outside the greenhouse, a weather station measures air temperature and relative humidity with a ventilated sensor, solar radiation, photosynthetic active radiation, rain detector, CO_2, wind direction, and wind speed. During the trials, several greenhouse climate variables were measured, especially air temperature, relative humidity, solar radiation, PAR, soil and cover temperature, and CO_2 concentration.

Irrigation was applied periodically throughout each day to each crop. The irrigation frequency was controlled using a demand tray system; fixed volumes

were applied. The demand tray system, using water-level sensors, is the most commonly used system for automatically activated irrigation of soilless crops in SE Spain. A water-level sensor is installed in a small water reservoir in which the water volume (and therefore the surface level) is in equilibrium with the substrate water content. When the water level in the reservoir decreases to the physical level of the sensor, as a result of crop uptake, irrigation is activated. The physical height of the sensor is adjusted by the grower on the basis of measured drainage volumes and experience. This method can be used once the crop root system is established. A microlysimeter was the system chosen to measure the transpiration, drainage and crop water loss measurements. The device consists of two electronic weighing scales connected to a personal computer. The first (150 kg 1 g, Sartorius) records the weight of a bag with six plants, and a support structure. The second weighing scale (20 kg 0.5 g, Sartorius), which follows the first, measures the drainage weight from the substrate bag. A more detailed description of the greenhouse was presented elsewhere [29].

3. System Modeling

The case of study presented in the previous section is used to investigate the performance of a DMPC technique which manages the optimal operation of the desalination plant to fulfill the water requirements of the crops while decreasing the thermal energy consumption of the MD modules. Thus, a model capable of accurately representing the behavior of both facilities is required.

3.1. SMD facility model

The model of the SMD facility can be divided in two different components coupled by means of a heat exchanger: (1) the heat generation system, formed by the solar field and the storage tank, and (2) the desalination unit. The model of the heat generation system was already presented in [16, 30]. In this work, in order to simplify the simulations, temperature profiles at the entrance of the hot side of the heat exchanger have been employed. These temperature

profiles were obtained simulating the model of the heat generation circuit with real meteorological data from PSA, similar to the ones used in this work, and using the operational strategy proposed in [16].

On the other hand, the heat exchanger was modeled with a first principles-based static model following the ideas proposed in [31]:

$$\mathrm{T}_{hs,out-m} = \mathrm{T}_{hs,in} - \eta_1 \cdot (\mathrm{T}_{hs,in} - \mathrm{T}_{cs,in}), \quad (1)$$

$$\mathrm{T}_{cs,out-m} = \mathrm{T}_{cs,in} + \eta_2 \cdot (\mathrm{T}_{hs,in} - \mathrm{T}_{hs,out-m}), \quad (2)$$

where:

$$\eta_1 = \frac{1 - e^{\theta}}{1 - \frac{\dot{m}_1 \cdot c_{p,1}}{\dot{m}_2 \cdot c_{p,2}} e^{\theta}}, \quad (3)$$

$$\eta_2 = \frac{\dot{m}_1 \cdot c_{p,1}}{\dot{m}_2 \cdot c_{p,2}}, \quad (4)$$

$$\theta = \alpha \cdot \mathrm{A}_{he} \cdot \left(\frac{1}{\dot{m}_1 \cdot c_{p,1}} - \frac{1}{\dot{m}_2 \cdot c_{p,2}} \right). \quad (5)$$

All variables and constants are defined in the nomenclature table in the appendices. The surface area of the heat exchanger (A_{he}) is 3.15 m^2. Moreover, as was presented in [16], a time delay and a first order filter have been added to each output of the model in order to add the required dynamic to fit experimental data. For the case of $\mathrm{T}_{cs,out-m}$ the time delay is 23 s and the representative time constant is 40 s, while for $\mathrm{T}_{cs,out-m}$ the time delay is 15 s and the time constant is 20 s.

As was mentioned in Section 2.1, two kinds of MD modules have been employed in this work. The models of the MD units consists on static equations obtained from experimental data, by means of the Response Surface Methodology (RSM). The model of the first module, the Solar Spring one (SS-1 and SS-2 in Fig. 1), was presented in [26] and it is given by:

$$\begin{aligned} \mathrm{D} = 10 \cdot (&-1.088 + 0.024 \cdot \mathrm{T}_{cs,out} - 0.018 \cdot \mathrm{T}_{feed} - 0.001 \cdot \mathrm{F} \\ &+ 0.00006 \cdot \mathrm{T}_{cs,out} \cdot \mathrm{F}), \end{aligned} \quad (6)$$

$$\triangle \mathrm{T} = -0.201875 + 0.1385 \cdot \mathrm{T}_{cs,out} - 0.158 \cdot \mathrm{T}_{feed} + 0.0049 \cdot \mathrm{F}. \quad (7)$$

The model of the Aquastill module (AQ-1 and AQ-2 in Fig. 1) was developed in [27] and it is described by the following equations:

$$\begin{aligned} \mathrm{D} = 24 \cdot (0.135 + 0.003 \cdot \mathrm{T}_{cs,out} - 0.0204 \cdot \mathrm{T}_{feed} - 0.001 \cdot \mathrm{F} \\ + 0.00004 \cdot \mathrm{T}_{cs,out} \cdot \mathrm{F}), \end{aligned} \tag{8}$$

$$\triangle \mathrm{T} = -0.739 + 0.078 \cdot \mathrm{T}_{cs,out} - 0.067 \cdot \mathrm{T}_{feed} + 0.0019 \cdot \mathrm{F}. \tag{9}$$

It should be mentioned that in equations (7) and (9), $\triangle$T is the temperature difference between the inlet evaporator channel temperature and the outlet temperature of the condenser channel of the MD module, and D is the distillate production. Notice that static models are used here because the MD modules have a fast dynamics. However, it can be observed that they are affected by the temperature coming from the heat generation circuit ($\mathrm{T}_{cs,out}$), and therefore, by its dynamics.

Finally, the feed flow rate is controlled by the pump 1 that supplies flow rates between 1600 and 2000 L/h. This feed flow rate is a shared resource between the four modules, and it is not enough to feed all the modules working at maximum flow rate (maximum flow rate of each module 600 L/h). Notice that this limitation could be a design decision, attending to the cost related to pump the sea water, and to the fact that the maximum thermal efficiency is achieved when the MD modules are run at the minimum feed flow rate, as will be shown in section 4.1. Then, valves V1, V2, V3 and V4, which vary their opening between 0 and 1, divert part of the flow into the corresponding module (see Fig. 1). Besides, V1 and V5, V2 and V6, V3 and V7, and V4 and V8, are opened or closed at the same time and at the same value, in order to maintain the same flow rate at the entrance of the two channels of each module.

3.2. Greenhouse model

A simplified pseudo-physical climate model completely described in [29] has been used for the purpose of this work. The state variables of the system are the inside air temperature ($\mathrm{T}_{a,int}$) and humidity ($\mathrm{H}_{a,int}$). The three main external systems interacting with the greenhouse are outside air, soil surface, and crop.

Thus, the greenhouse air temperature ($\mathrm{T}_{a,int}$) can be modeled using the following balance:

$$c_{p,a}\rho_a \frac{\mathrm{V}_g}{\mathrm{A}_{ss}} \frac{d\mathrm{T}_{a,int}}{dt} = Q_{sol,a} + Q_{cnv,cv-a} + Q_{cnv,ss-a} - Q_{ven} - Q_{trp,cr}, \quad (10)$$

where $Q_{sol,a}$ represents the radiative flux heating the inside air through the cover, $Q_{cnv,cv-a}$ is the convective flux with the cover, $Q_{cnv,ss-a}$ is the convective flux with the soil surface, Q_{ven} is the heat lost by natural ventilation and infiltration, and $Q_{trp,cr}$ is the latent heat effect of the crop transpiration. The remaining variables are presented in Nomenclature (see the appendices).

Moreover, greenhouse inside absolute humidity ($\mathrm{H}_{a,int}$), which is the amount of water vapour in the greenhouse air, is modeled based on a vapour mass balance [29]:

$$\rho_a \frac{\mathrm{V}_a}{\mathrm{A}_{ss}} \frac{d\mathrm{H}_{a,int}}{dt} = \dot{M}_{trp,cr} + \dot{M}_{hum} - \dot{M}_{dehum} - \dot{M}_{vent,int-ext}, \quad (11)$$

where $\dot{M}_{trp,cr}$ is the crop transpiration flux, that is related with the amount of water lost by plants in the transpiration process which must be recovered by irrigation, $\dot{M}_{hum}$ is the water flux provided by the humidification system, $\dot{M}_{dehum}$ is the water flux removed by the dehumidifcacion system, and $\dot{M}_{vent,int-ext}$ is the outflow by natural ventilation and infiltration. Notice also that the remaining variables are presented in Nomenclature (see the appendices).

It should be commented that the area of cultivation in the model was fixed at 308 m^2 in order to scale the water consumption of the greenhouse with the production of the four MD modules.

4. Control system

The main idea is to develop a control algorithm able to make an optimal distribution of the feed flow rate between the MD modules, according to the water demand of the greenhouse and the thermal efficiency of the MD modules at each instant. For this purpose, DMPC controllers become an attractive approach since in industrial applications the number of MD modules required

increases significantly, and the application of a centralized controller could be very difficult in terms of computational power and communications.

In what follows, the performance of each MD module with respect to distillate production and thermal efficiency is showed and analyzed. Based on this analysis, first, the centralized controller is formulated, and then, the distributed approach is presented. After that, the simulation results and some conclusions are presented.

4.1. Optimal operation of the MD modules

Before presenting the development of the control system, it is important to analyze and even visualize the performance of each module, in order to clarify the way in which the control system has been designed. Two of the most important metrics used to describe the performance of membrane distillation modules are the distillate production and the thermal efficiency. Thus, in this section, 3D response surface plots of each module are presented, showing the behavior of the two metrics with respect to the evaporator inlet temperature and the feed flow rate, the two most important variables influencing them.

On the one hand, the value of the distillate production can be directly obtained, just measuring the quantity of distillate produced at each sample time. On the other hand, the thermal efficiency of the process must be estimated using one of the performance metrics presented in the literature. In this case, the Specific Thermal Energy Consumption (STEC) has been selected [28, 27, 26]. This metric provides the quantity of thermal energy required to produce a volume unit of distillate, and it can be calculated as follows:

$$\text{STEC (kWh/m}^3) = \frac{\mathrm{F} \cdot \rho_{feed} \cdot c_{p,2} \cdot (\mathrm{T}_{cs,out} - \mathrm{T}_{cs,in})}{c_f \cdot \mathrm{D}}. \tag{12}$$

Notice that all the variables involved in the previous equation are defined in Nomenclature.

Fig. 5 shows the 3D response surface plots. Regarding the distillate production, it can be observed that the maximum value is obtained when operating at maximum feed flow rate and evaporator inlet temperature for both modules (see

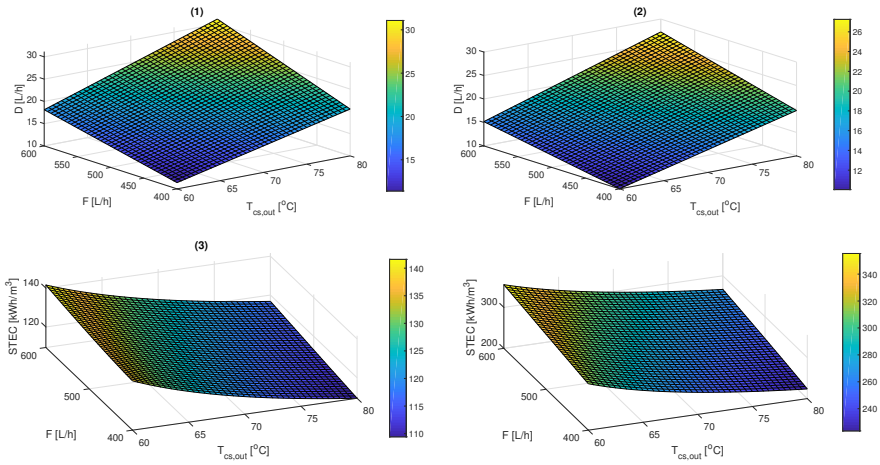

Figure 5: 3D response surfaces. (1) Distillate production of Aquastill module, (2) distillate production of Solar Spring module, (3) STEC of Aquastill module, and (4) STEC of Solar Spring module

Fig. 5-1 and Fig. 5-2). However, in the case of STEC, which must be minimum to obtain a higher thermal efficiency in the process, the optimal operating points are reached in both cases working at maximum evaporator inlet temperature and minimum feed flow rate (see Fig. 5-3 and Fig. 5-4). In addition, comparing the two modules, it can be seen that the Aquastill module has a higher distillate production and thermal efficiency than the Solar Spring one. So, to summarize, the most important conclusions which will be the basis for the development of the control system are: i) the evaporator inlet temperature should be the highest possible (notice that it depends on solar irradiance) to obtain optimal performance, ii) contrary operating conditions are required in the feed flow rate to maximize the distillate production and thermal efficiency in both modules, and iii) the Aquastill module produces more distillate and it is more efficient than the Solar Spring one.

4.2. Centralized control approach

MPC is a control technique widely used in both industry and academy. MPC can include, but not only, optimal control, dead time, multivariable processes

and uses the future setpoints if they are available [32]. By using a finite receding control horizon strategy it also allows to deal with constraints and nonlinear processes. MPC controllers use the following structure and features (see Fig. 6):

- Explicit use of a process model to predict the process behaviour in the future $\hat{y}(t+j|t)$.
- Minimization of a cost function with the aim to calculate the control signal $u(t|t)$. This objective function usually tries to maintain the process as close as possible to a determine reference $w(t+j|t)$.
- Use of a finite receding control horizon which means that a set of control signals is calculated for the whole horizon $(u(t|t), u(t+1|t), ..., u(t+N_u-1|t))$ but only the first control signal is applied and the rest are rejected.

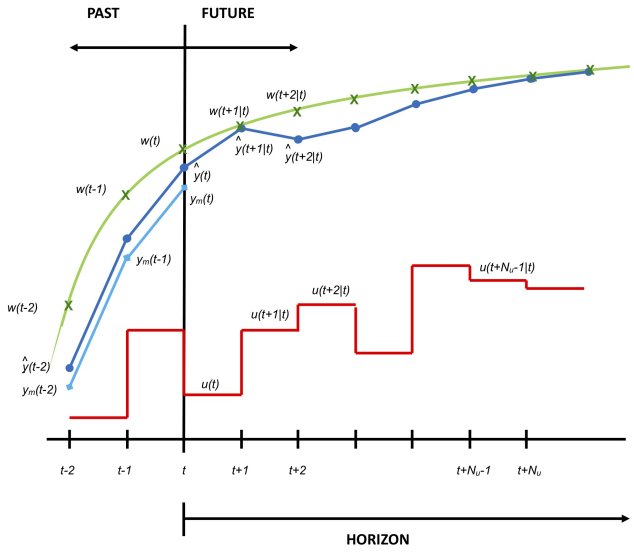

Figure 6: MPC strategy.

The main differences among MPC strategies lie in both, the process model and the noise model, and the cost function. These differences can cause distinct behaviours in a feedback loop.

In this way, due to many advantages when compared to other control strategies [32], the MPC strategy has been chosen as the most suitable one for this work. Therefore, assuming a prediction and control horizons with length N and N_u, respectively, the cost function for a particular system can be formulated as follows:

$$J = \sum_{j=1}^{N} \delta \cdot [\hat{y}(t+j|t) - w(t+j|t)]^2 + \sum_{j=0}^{N_u-1} \lambda \cdot [\Delta u(t+j)]^2, \tag{13}$$

where the prediction of the system output and the desired reference, $\hat{y}(t+j|t)$ and $w(t+j|t)$ respectively, are estimated for sample time $t+j$ with the information available at sample time t. On the other hand, $\Delta u(t+j)$ is the variation of the control action at sample time $(t+j)$ whereas δ and λ are weighting factors that penalize the future tracking errors and control efforts, respectively, along their horizons.

Regarding constraints, mainly three kinds of constraints can be found that concern to system outputs and control actions:

$$\Delta u_{min} \leq \Delta u(t) \leq \Delta u_{max}, \forall t \geq 0, \tag{14a}$$

$$u_{min} \leq u(t) \leq u_{max}, \forall t \geq 0, \tag{14b}$$

$$y_{min} \leq y(t) \leq y_{max}, \forall t \geq 0. \tag{14c}$$

In the previous equations, the first constraint, Eq. (14a), limits the control effort in order to avoid abrupt changes in the actuator that may cause any disruption. The second one, Eq. (14b), makes reference to physical hard constraints of the actuator. Finally, the third constraint, Eq. (14c), gives the lower and the upper limit, y_{min} and y_{max} respectively, of the output variable (also applicable to predicted future values).

In this work, the cost function presented in Eq. (13) has been modified according to the problem at hand. Thus, for the centralized control approach,

the cost function is given by:

$$J = \sum_{j=1}^{N} \zeta \cdot \hat{y}_{STEC}(t+j|t) + \sum_{j=1}^{N} \delta \cdot [w_{tank}(t+j) - \hat{y}_{tank}(t+j|t)] + \sum_{j=0}^{N_u-1} \lambda \cdot \Delta u(t+j), \tag{15}$$

where $\zeta = (1\text{-}\delta)$, $\hat{y}_{STEC}$ is the mean value of the STEC of the four MD modules, $\hat{y}_{tank}$ is the level of the tank and w_{tank} is the minimum allowed level of the tank. In addition, it should be remarked that the set of inputs $\boldsymbol{u}$ is composed by the feed flow rate of each of the MD modules, what means according to Fig. 1, $\boldsymbol{u}$=[$\mathrm{F_{AQ-1}}$ $\mathrm{F_{SS-1}}$ $\mathrm{F_{SS-2}}$ $\mathrm{F_{AQ-2}}$].

4.3. Distributed control

In this work, a system composed by M subsystems or agents, i.e, the MD modules, is considered. Then, for each agent i, Eq. (15) can be rewritten as follows:

$$J_i = \sum_{j=1}^{N} \zeta \cdot \hat{y}_{STEC}(t+j|t) + \sum_{j=1}^{N} \delta \cdot [w_{tank}(t+j) - \hat{y}_{tank}(t+j|t)] + \sum_{j=0}^{N_u-1} \lambda_i \cdot \Delta u_i(t+j). \tag{16}$$

Regarding to the constraints, as has been pointed out before, each agent i can have its own constraints as it is shown in Eqs. (14). However, this work is concerned with a plant that is formed by interconnecting M dynamic subsystems which share a common resource. Let $\mathcal{M} = \{1, \ldots, M\}$ be the set of agents or subsystems. In this case, the shared resource is the water flow supplied from the feed water tank and, to impose a limit to it, a new constraint which couples all the subsystems must be considered. Such a constraint can be defined as follows:

$$\sum_{i=1}^{M} u_i(t+j) \leq b, \, \forall j = 1, \ldots, N, \tag{17}$$

where b is the allowable resource. For the problem at hand, this constraint is related to the total feed water flow supplied from the feed water tank to the whole system, which could be limited by design decisions as previously mentioned. Then, the optimization problem for the whole system, that is, including

the M subsystems, can be formulated as follows:

$$P(t): \quad \min \quad f(\Delta u_i) = \sum_{j=1}^{N} \zeta \cdot \hat{y}_{STEC}(t+j|t) + \\ + \sum_{j=1}^{N} \delta \cdot [w_{tank}(t+j) - \hat{y}_{tank}(t+j|t)] + \sum_{i=1}^{M} \sum_{j=0}^{N_u-1} \lambda_i \cdot \Delta u_i(t+j) \quad (18a)$$

$$\text{s.to}: \sum_{i=1}^{M} u_i(t+j) \leq b, \forall j = 1, \ldots, N \quad (18b)$$

$$u_{min} \leq u_i(t+j) \leq u_{max}, \forall j = 1, \ldots, N. \quad (18c)$$

Notice that, the optimization problem $P(t)$ defined by Eq. (18) would consist of a set of M decoupled subproblems if it were not for the coupling constraint in Eq. (18b). The first term, y_{STEC} in Eqs. (15) and (16), which is related to the mean STEC of the four MD modules, is added to maximize the thermal efficiency of the operation of the SMD plant. On the other hand, the tank level, y_{tank}, should not have a value lower than 1500 L, that is, $y_{tank} \geq 1500$, this value has been chosen since it ensures the supply of the greenhouse for two days without MD production, as the average consumption per day is around of 750 L. However, setting this constraint as a hard constraint makes the optimization problem unfeasible, thus, a soft constraint has been added to the second term of both Eqs. (15) and (16), where w_{tank} is set to 1500 L for the whole prediction horizon.

It should be remarked that the two terms involved in the objective function require contrary operating conditions, since to maximize the thermal efficiency, the MD modules must be run at the minimum feed flow rate value, whereas to maximize the distillate production to increase the tank level, the MD modules must be fed at the maximum flow (see Section 4.1). Nevertheless, not always the two objectives have to be maximized at the same time, so the following

function is used to set the weighting factors ζ and δ:

$$\zeta = \begin{cases} 0 & if \quad x \leq c, \\ d \cdot x + e & if \quad c < x < f, \\ 1 & if \quad x \geq f. \end{cases} \tag{19}$$

In this function, x is the level of the tank at instant time t, c and f are specific levels of the tank, and d and e are the factors of a first order polynomial. It should be remembered that δ= (1-ζ). Therefore, if the tank level is below c, only the part related with increasing the level of the tank is considered in the objective function. Conversely, if the level of the tank is above f, the objective function is aimed at maximizing the STEC, whereas if the level of the tank is between c and f the two objectives are considered, calculating the weighting factors by means of a first order polynomial, thus obtaining a soft transition between the two objectives and avoiding chattering problems in the control signals.

Additionally, it should be commented that, among the set of constraints presented in Eq. 18, only the constraint related to the physical limitations of the actuators has been included in the problem, since it is the only limitation imposed by the system as the feed flow rate of the MD modules must be between 400 and 600 L/h, which is u_{min} equal to 400 and u_{max} equal to 600 L/h.

The procedure that each agent or subsystem i must perform at each iteration l within a sample period t is the following [24]: read the decisions of the neighbors, coordinate its iterations, and calculate its own control actions by solving problem $P(t)$. To this aim, the agent will need to receive from the upstream agent the residual feed water flow and from the downstream agent, the previous control signal $u_{i+1}(t-1)$, the latest prediction for output $\hat{y}_{i+1}(t)$, and the latest control increment $\Delta u_{i+1}(t)^l$.

Upon satisfying a convergence criterion, i.e. the difference between the results of two iterations is less than a minimum established threshold ε, or reaching

the maximum number of iterations σ, the obtained control values are applied in the valves, the horizon is shifted to the next sample time, and the process is repeated. This procedure is given in pseudo-code in Algorithm 1.

Algorithm 1: Distributed optimization performed by agent i during the iteration l at sample time t

if agent i cannot revise its decisions in iteration l **then**

$\Delta u_i(t)^{l+1} = \Delta u_i(t)^l$

else

- Agent i receives the available feed water flow from the upstream agent $i-1$ and $\Delta u_{i+1}(t)^l$ from the downstream agent $i+1$;
- Agent i solves problem $P(t)$ to obtain $\Delta u_i(t)^{l+1}$ and the prediction of available feed water flow;

Finally, to solve this optimization problem, function *fmincon* which can be found in the MATLAB *Optimization Toolbox* [33] has been used.

5. Results and discussion

This section shows the results of the simulation experiments carried out to evaluate the effectiveness of the proposed control strategy. The schematic diagrams showing how the simulations were performed for the centralized and distributed approaches are presented in Figs. 7 and 8. As can be seen, the experimental campaign was performed using temperature profiles of the heat generation circuit of the SMD plant ($T_{hs,in}$ in Figs. 7 and 8), as mentioned above. These temperature profiles were connected with a simulator that emulated the behavior of the MD modules and the greenhouse by using the models presented in Section 3. For simulating the model of the greenhouse, meteorological data from Experimental Station of Cajamar Foundation were employed, on the day July 20, 2017. In addition, in the simulations, both control approaches used linearized models of the system around the operating point $\boldsymbol{u}$ for predicting $\hat{y}_{STEC}$

and $\hat{y}_{tank}$, which are obtained at each sampling time by means of the technique presented in [34]. Notice that the linear models are calculated only once in the distributed approach (see Fig. 8) since the strategy has been implemented in only one computer, but in real implementations they must be calculated as many times as the number of agents included in the optimization problem. It should be remarked that the linearized models have been used in the controllers instead of the nonlinear ones due to the high computational effort required for solving the optimization problem with the nonlinear ones. In this way, the controllers have to cope with uncertainties caused by disturbances, modeling errors and neglected dynamics. Besides, the use of two different kinds of MD modules, with different behaviours, increases the complexity of the automatic operation.

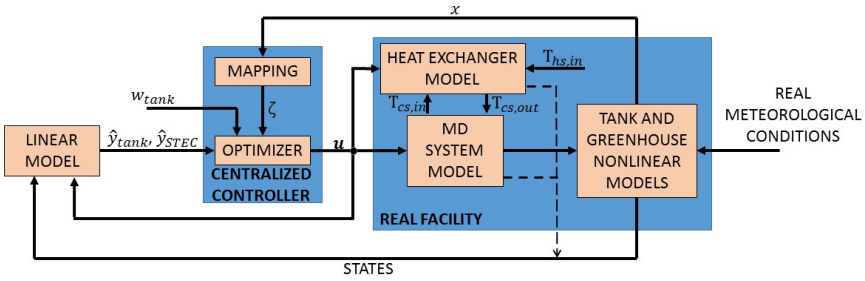

Figure 7: Centralized approach simulation scheme.

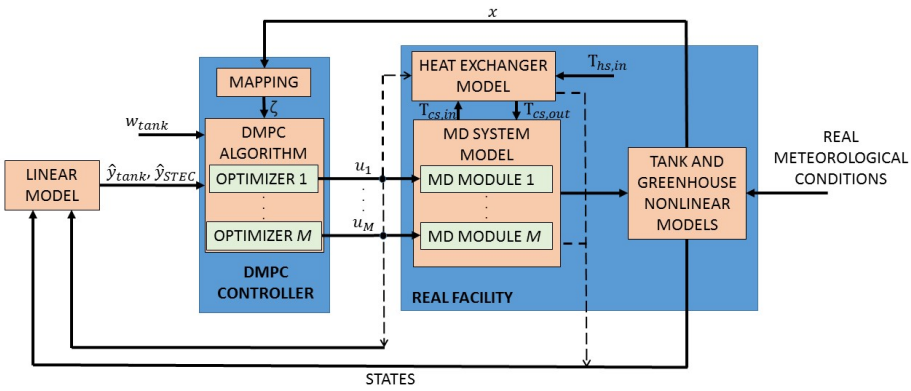

Figure 8: Distributed approach simulation scheme.

In the experiments, the maximun feed flow rate provided by pump 1 (see Fig. 1) was limited to 2000 L/h (as mentioned in Section 3.1), that is b=2000 L/h, trying to mimic the conditions that would occur in industrial cases. It must be bear in mind that in this case of study only four modules are required to fulfill the water requirements of the pilot greenhouse. This pilot configuration was chosen since it accurately represents practical situations, and facilitates the visualization of the results. However, when considering greenhouses of industrial size, the number of commercial MD modules considerably augments, and the feed flow rate may be limited either by design (as mentioned in Section 3.1) or operational constraints, requiring adequately control algorithms to deal with these situations.

The MD modules come into operation when the evaporator inlet temperature is higher than 60 °C (low operational limit of the modules), and are turned off when it is lower than 60 °C. This strategy has been implemented using the procedure presented in [16], in which mean values are used instead of instant ones for checking, thus avoiding chattering problems. In this way, the MD modules are started after reaching 60 °C, specifically at 63.6 °C with the condition used in the simulations. Moreover, as initial point, valves V1, V2, V3 and V4 were fixed at 0.5, what corresponds to a feed flow rate of 475 L/h in each MD module, and the initial level of the distillate tank was 1600 L.

Regarding the controller set up, the sampling time was 10 minutes, selected taking into account the representative time constants of the crop transpiration inside the greenhouse and that of the temperature of the heat generation circuit of the SMD plant. The horizons were selected considering traditional recommendations in MPC controllers, $N_u \ll N$, and N larger enough to contemplate the transient part of the response, thus ensuring a stable closed loop performance. The final values were $N = 6$ and $N_u = 2$. In the same way, λ was fixed at 0.1, which was chosen after exhaustive simulation until obtaining the desired closed loop response. Moreover, σ was fixed to 200. This parameter is related to the maximum number of iterations of the DMPC algorithm at each sample time. In this way, it was chosen big trying that the DMPC algorithm

stops when reaching the threshold criterion instead of this one.

On the other hand, c was fixed to 1510 L whilst g at 1620 L. The first value was chosen since c should be slightly higher than the minimum tank level (1500 L), thus allowing to the controller to take into consideration as much as possible the thermal efficiency term in the objective function. Conversely, g must be chosen to allow a soft change between the two objectives included in the objective function. Thus, comprehensive simulations were carried out with several values of g, showing that with values of g closer to the ones of c, abrupt changes in the control signals can be obtained which can cause chattering problems. Besides, the thermal efficiency index was not considerable improved. The factors of the polynomial were fixed at [d, e]=[0.0091, -13.6383], which were obtained by interpolating between c and g. Finally, the controller was implemented in a PC with Intel Core i5-6500T CPU 2.50 GHz with 8 GB of RAM in MATLAB code.

The simulation results are presented as follows: i) the convergence of the DMPC approach to optimal solutions is checked by comparing the results obtained with the DMPC algorithm with those of the centralized approach, ii) the use of the DMPC approach is justified, by scaling the problem to plants of industrial size, and measuring the maximun time spent by the DMPC and the centralized formulations for solving the control problem, and iii) the benefits of the automatic operation is presented by comparing its performance with a non-optimal management of the facility, a manual operation.

5.1. Convergence of the DMPC approach to optimal solutions

This section presents the simulations performed in order to check the convergence of the DMPC approach to optimal solutions. It should be commented that the distributed controller is an approximation of the centralized one, and the theoretical optimal solution must be the same that the one obtained with the centralized algorithm. For this reason, the same test has been carried out with the centralized and the distributed algorithm in order to graphically and quantitatively compare both approaches.

The results of the simulations for the centralized and distributed controllers are shown in Figs. 9 and 10 respectively. Notice that, both the inlet temperature of the heat exchanger for the hot side (see Figs. 9-1 and 10-1) and the greenhouse consumption (see Figs. 9-4 and 10-4) depend directly on the solar irradiance. Although the global irradiance curve has not been included in the graphics for the sake of simplicity, in Almería, in a Summer day, the solar midday is around 2.00 pm. In this way, it can be observed how the water consumption of the greenhouse (see Figs. 9-4 and 10-4) is maximum around this instant time. However, the temperature at the inlet of the heat exchanger is maximum later due to the volume of water accumulated in the storage tank placed between the solar field and the heat exchanger (see Figs. 9-1 and 10-1). Consequently, the distillate production of the four MD modules reaches the maximum also later since it depends on this temperature (see Figs. 9-4 and 10-4).

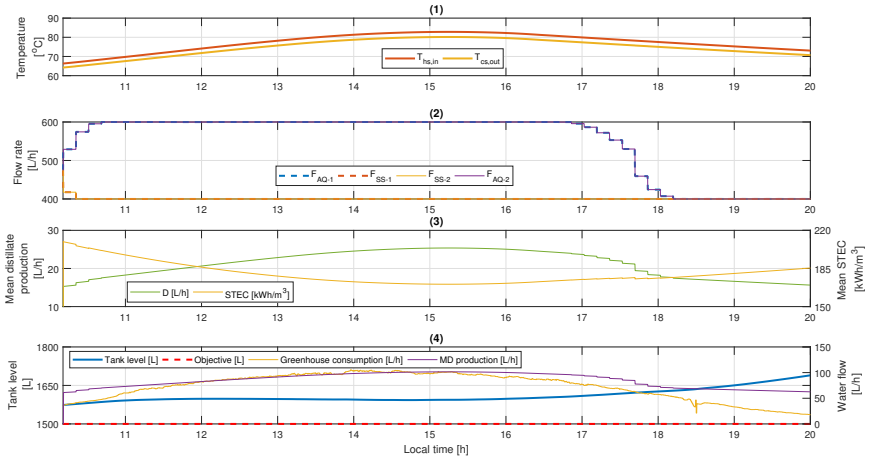

Figure 9: Results obtained with the centralized approach. (1) Temperature at the entrance of the heat exchanger, hot side ($T_{hs,in}$), and temperature leaving the cold side of the heat exchanger ($T_{cs,out}$), (2) MD modules feed flow rates (F_{AQ-1}, F_{SS-1}, F_{SS-2}, and F_{AQ-2}) (3) mean distillate production of the four MD modules (D) and mean STEC (STEC), and (4) tank level, objective (minimum allowed level of the tank), greenhouse water consumption, and MD production.

As pointed out before, the automatic operation starts when the temperature

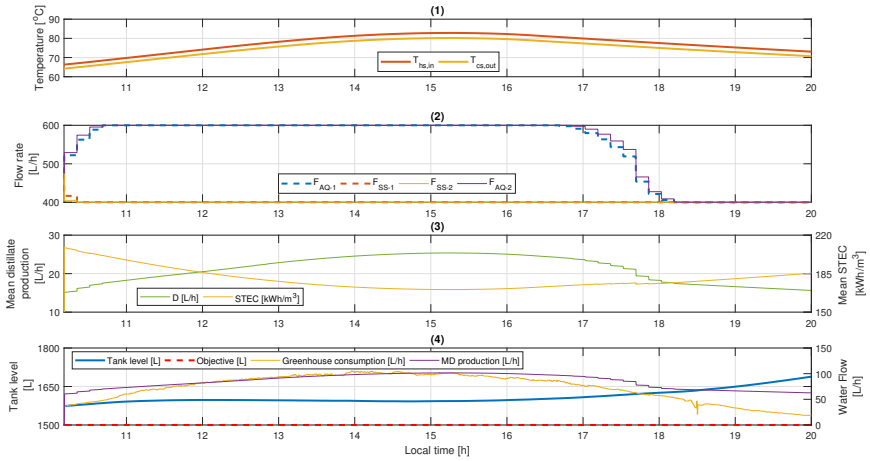

Figure 10: Results obtained with the distributed approach ($\varepsilon = 10^{-4}$). (1) Temperature at the entrance of the heat exchanger, hot side ($T_{hs,in}$), and temperature leaving the cold side of the heat exchanger ($T_{cs,out}$), (2) MD modules feed flow rates (F_{AQ-1}, F_{SS-1}, F_{SS-2}, and F_{AQ-2}) (3) mean distillate production of the four MD modules (D) and mean STEC (STEC), and (4) tank level, objective (minimum allowed level of the tank), greenhouse water consumption, and MD production.

at the inlet of the evaporator channel of each MD module is higher than 60 °C (see Figs. 9-1 and 10-1). This condition is checked using the model of the heat exchanger, as was presented in [16]. In this moment the tank level is 1575 L (notice that the greenhouse consumes water before the modules are started), therefore, in the objective function both the distillate production and the STEC objectives are taken into account with the weighting factors calculated by means of the polynomial. For this reason, in the first sampling time, the controllers increase the feed flow rate diverted for the Aquastill modules, and decrease that delivered for the Solar Spring ones (see Figs. 9-2 and 10-2). This procedure is continued in the following sampling times, until saturating the control signals. In this way, the MD modules which have a higher distillate production and a lower STEC (Aquastill ones) are fed at the maximun feed flow rate (600 L/h), whereas the Solar Spring modules are feed at minimum fed flow rate (400 L/h). With this optimal distribution, the mean distillate production of the four MD

modules is augmented, while the mean STEC is decreased (see Figs. 9-3 and 10-3), thus achieving optimal performance and maintaining the desired level in the distillate tank. Around 16 h, the water consumption of the greenhouse decreases and the level of the tank increases (see Figs. 9-4 and 10-4). Thus, in the objective function, the weighting factor of the part related with the STEC augments in accordance with the polynomial, and the feed flow rates of the Aquastill modules are reduced by the controller (see Figs. 9-2 and 10-2). Around 17.30 h, the level of the distillate tank is over 1620 L, what produces that only the part related with the STEC is considered in the objective function. Accordingly, the feed flow rates of the Aquastill modules are decreased faster until reaching the minimum value (see Figs. 9-2 and 10-2), in order to increase the thermal efficiency of the operation (see Figs. 9-4 and 10-4).

Controller	STEC [kWh/m^3]	Distillate [L]
No	190.35	1719.00
MPC	180.56	1733.82
DMPC ($\varepsilon = 10^{-1}$)	180.57	1733.80
DMPC ($\varepsilon = 10^{-2}$)	180.57	1733.80
DMPC ($\varepsilon = 10^{-3}$)	180.57	1733.80
DMPC ($\varepsilon = 10^{-4}$)	180.56	1733.81
DMPC ($\varepsilon = 10^{-5}$)	180.56	1733.82

Table 1: Comparison between an operation with the centralized MPC controller, an operation with several DMPC configurations varying ε, and an operation without controller, with static setpoint in valves V1, V2, V3 and V4 equal to 0.5.

Notice that the performance of both controllers is very similar, and the differences between them can be observed only in the control signals during the transients. They are caused by the way in which the control signals are calculated by the DMPC algorithm (see Algorithm 1). However, these differences hardly affect the overall performance of the system in terms of distillate production and thermal efficiency (see Figs. 9 and 10). This fact can be quantitatively

checked in table 1, in which the mean STEC of the operation and the distillate produced by the four MD modules are summarized for the centralized MPC case, and for several DMPC cases with different values of ε. All the simulations were performed using the same operating conditions than the ones employed in the Figs. 9 and 10. Thus, as can be seen in table 1, for a ε equal to 10^{-5}, the same results in terms of STEC and distillate production than in the centralized approach are obtained. In the same way, when increasing ε, the results are still almost the same, until reaching the value of 10^{-1}, which is the limit. With this value, the controller still provides a stable response and an optimal distribution of the feed flow rate. However, with ε higher than 10^{-1}, the algorithm converges to solutions distant from the optimal ones.

5.2. Justification of the use of the DMPC approach

One of the main advantages of the DMPC approach is that the optimization problem that must be solved by each agent is simple and small, independently of the number of agents involved in the system. This fact influence in the time spent by the algorithm to reach a stationary solution. In this way, the time spent in solving the optimization problem with the centralized and the distributed approach has been also analyzed. Notice that the facility used in this work is a small pilot plant, so that, the centralized formulation of the problem is favored. Conversely, if facilities of industrial size are considered, the number of MD modules required to fulfill the water requirements increases considerably, and therefore, the computation time. For this reason, several simulations have been carried out increasing the number of hectares of crops that must be irrigated by the SMD plant, thus allowing to analyze the maximum time spent for each algorithm in solving the optimization problem in a sampling time (see Fig. 11).

As can be seen in Fig. 11, and as it was pointed out before, the centralized approach is slightly favoured when considering facilities of small size (i.e 1 or 2 hectares). Conversely, if considering large crops surfaces, the time spent by the centralized approach exponentially increases making that with 16 ha the time is almost equal to the sampling time, so that, the algorithm does not provide an

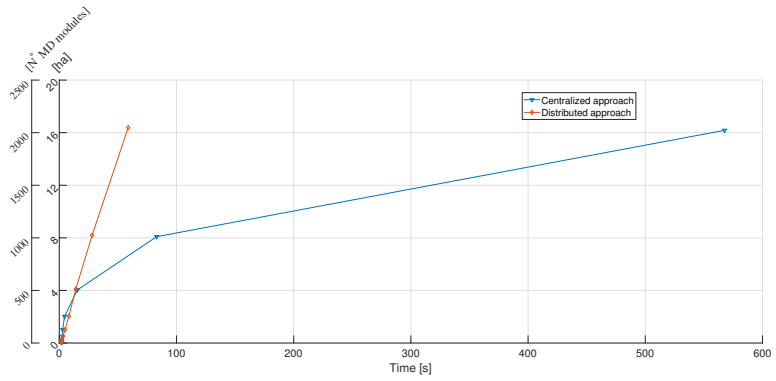

Figure 11: Maximum time spent for each algorithm in solving the optimization problem in a sampling time depending on the number of hectares that must be irrigated. The number of MD modules required for each case is also showed. These simulations have been performed fixing $\varepsilon = 10^{-4}$ in the distributed algorithm.

optimal solution within the required time period. Notice that the time required by the distributed approach also augments depending of the number of hectares but in a linear way, thus allowing to obtain optimal solutions for large facilities in the required time period, which is one of the main advantages of this algorithm and one of the main reasons for choosing this algorithm for this application. It is also important to remark that, the expansion of the algorithm for larger plants is very easy, as the introduction of a new agent in the problem requires changes only in the neighboring agents, without reprogramming the entire algorithm.

In addition, it should be remarked that, apart from the benefits achieved in the time spent in solving the optimization problem, the DMPC approach stands out by the following general advantages of these kind of algorithms: i) the risk of failure is reduced because the system does not depend on a centralized controller, so that, the supply of the greenhouse is not compromised, ii) the communication between agents is easier, because each agent is connected only with its neighbors, what would simplify the communication network in an industrial facility.

5.3. Benefits of the optimal operation

The results obtained with the MPC controllers were compared with an operation using static control signals in valves V1, V2, V3 and V4 of 0.5. To perform this comparison, the same operating conditions than those considered in section 5.1 were employed. The results of this simulation are presented in table 1. The mean STEC for an operation with static values in the valves was 190.35 kWh/m^3, whereas the total distillate production was 1719 L. When a controller was used for making an optimal distribution of the feed flow rate, almost 10 kWh (around 5 %) less of thermal energy was required to produce 1 m^3 of distillate, while the total distillate production increased in more than 14 L.

To analyse the energy savings achieved by means of the proposed MPC approach, the results obtained in this case of study have been extrapolated to industrial cases. According to the studio performed in [35], a tomato crop growth has a water requirement of 4110 m^3/ha during a season. In addition, if the water consumed by the humidification system is considered (200 L/m^2 in a season [36]), the water necessities increase even more. In Fig. 12 the absolute thermal energy savings have been plotted for the case of a tomato crop growth (considering also the humidification system) depending of number of hectares that must be irrigated.

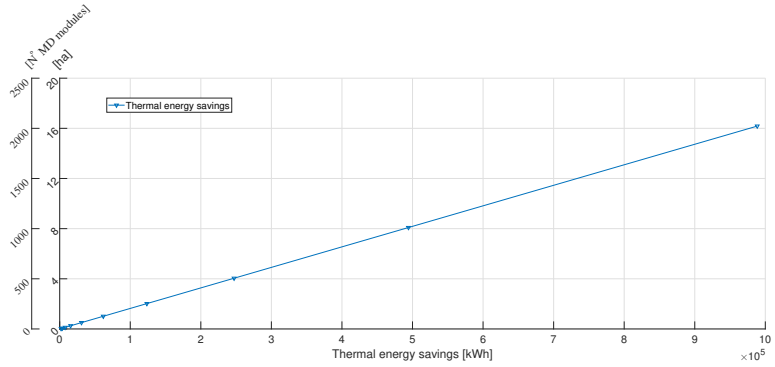

Figure 12: Absolute energy savings in a season depending on the number of hectares that must be irrigated. The number of MD modules required for each case is also showed.

It should be pointed out that the improvements achieved by means of the control system are almost constant independently of the operating conditions, since the worst operating conditions are reached when there are passing clouds or the level of the global irradiance is low. However, an adequate control system over the solar field [16] and the appropriate use of an storage system reduce the effect of irradiance disturbances over the MD system. It should be also remarked that these savings could be considered in the design phase, allowing to reduce the costs associated with the oversizing of the thermal energy sources. In the same way, it could be very relevant in the daily operation, specially in the cases in which non-renewable sources are used (i.e boilers), since a considerable amount of fuel, biomass, multi-fuel, or any type of power can be saved, thus reducing the daily operating costs.

6. Conclusions

This paper has addressed the optimal management of a distributed energy system composed of a solar membrane distillation facility and a greenhouse, connected by means of a buffer system. The scenario comprises the generation of thermal energy using flat plate solar collectors, and the distribution of this energy between the different MD modules included in the SMD plant to fulfill the greenhouse water demand.

A DMPC has been employed for the optimal operation of the plant. In this control approach, each agent solves a simple and easy MPC problem, exchanging information only with the neighborhood agents, and making an optimal distribution of the available resources as a whole. Besides, in the cost function defining the optimization problem two weighted objectives were considered. The first one is aimed at maximizing the thermal efficiency of the SMD system, which is identified as one of the main weak point of this technology. The second one is related to the level of the intermediate buffer located between SMD facility and the greenhouse, which must be higher than a specific minimum value to

guarantee the water supply to the greenhouse. Based on these objectives, the control algorithm computes the optimal distribution of the feed flow rate for each MD module.

Simulation experiments using real meteorological data from Plataforma Solar de Almería and Experimental Station of Cajamar Foundation were performed to evaluate the proposed control technique. These experiments focused on evaluating the controller when the resources are limited, situations that could be reached in industrial facilities due to operational or design constraints.

The results show that the DMPC controller is suitable for managing these kind of facilities, improving the thermal efficiency of the facility by 5 % in comparison with a manual operation, and maintaining the level of the intermediate tank above the objective. These thermal energy savings mean that for an industrial size cultivation area, i.e 8 ha, 49430 kWh/season less of thermal energy is required, what could be very relevant in both the design phase and the daily operation, specially when considering also non-renewable sources to feed the MD modules. Besides, the results were also compared with a centralized controller, showing that the performance of both approaches is very similar. However, the computational effort and the communications are considerably reduced with the distributed approach, what implies that in industrial cases, in which the number of MD modules included in the plant and therefore the number of agents involved in the optimization problem significantly increases, the problem can only be solved by using the DMPC approach.

Acknowledgements

This work has been funded by the National R+D+i Plan Projects DPI2014-56364-C2-1/2-R and DPI2017-85007-R of the Spanish Ministry of Science, Innovation and Universities and ERDF funds.

Nomenclature

Symbol	Description	Units
A	Surface area	m^2
c_f	Conversion factor	$3.6{\cdot}10^6$ s·W/(h·kW)
c_p	Specific heat capacity	J/(kg·°C)
D	Distillate production	L/h
F	Feed flow rate	L/h
H	Absolute humidity	kg water/kg air
$\dot{m}$	Mass flow rate	kg/s
$\dot{M}$	Mass flow rate per square meter	kg/(s·m^2)
Q	Heat flux	W/m^2
T	Temperature	°C
V	volume	m^3
α	Heat exchanger transfer coefficient	689.30 W/(m^2·K)
δ	Weighting factor for the tracking error	-
ΔT	Temperature difference	°C
ε	Convergence factor	-
ζ	Weighting factor for the STEC	-
η	Auxiliary factor for the calculation	-
	of the outlet heat exchanger temperatures	-
θ	Heat exchanger auxiliary factor	-
λ	Weighting factor for the control action	
ρ	Density	kg/m^3
σ	Maximum number of iterations	-

Subscript	Description
a	Air
cnv	Convective
cr	Crop
cs, in	Input at the cold side of the heat exchanger
cs, out	Output at the cold side of the heat exchanger
cv	Cover
$dehum$	Dehumidification
ext	Exterior
$feed$	Feed MD water
g	Greenhouse
he	Heat exchanger
hs, in	Input at the hot side of the heat exchanger
hs, out	Output at the cold side of the heat exchanger
hum	Humidification
i	ith MD module in the plant
int	Interior
m	Model output
sol	Solar
ss	Soil surface
trp	Transpiration
ven	Ventilation
1	Relative to the hot side of the heat exchanger (demineralized water fluid)
2	Relative to cold side of the heat exchanger (sea water fluid)

References

[1] Garcia-Caparros P, Contreras JI, Baeza R, Segura ML, Lao MT. Integral management of irrigation water in intensive horticultural systems of

Almería. Sustainability 2017;9(12):2271. doi:10.3390/su9122271.

[2] Cazcarro I, Duarte R, Martín-Retortillo M, Pinilla V, Serrano A. Water scarcity and agricultural growth in Spain: from curse to blessing. Natural Resources and Economic Growth: Learning from History Routledge, London 2015;:339–61.

[3] Sánchez-Molina JA, Rodríguez F, Guzmán J, Ramírez-Arias J. Water content virtual sensor for tomatoes in coconut coir substrate for irrigation control design. Agricultural Water Management 2014;151(31):114–25. doi:10.1016/j.agwat.2014.09.013.

[4] Burn S, Hoang M, Zarzo D, Olewniak F, Campos E, Bolto B, et al. Desalination techniques-A review of the opportunities for desalination in agriculture. Desalination 2015;364:2–16. doi:10.1016/j.desal.2015.01.041.

[5] Díaz FJ, Tejedor M, Jiménez C, Grattan SR, Dorta M, Hernández JM. The imprint of desalinated seawater on recycled wastewater: Consequences for irrigation in Lanzarote island, Spain. Agricultural Water Management 2013;116:62–72. doi:10.1016/j.agwat.2012.10.011.

[6] Martínez-Álvarez V, Martin-Gorriz B, Soto-García M. Seawater desalination for crop irrigation: A review of current experiences and revealed key issues. Desalination 2016;381:58–70. doi:10.1016/j.desal.2015.11.032.

[7] Amy G, Ghaffour N, Li Z, Francis L, Linares RV, Missimer T, et al. Membrane-based seawater desalination: Present and future prospects. Desalination 2017;401:16–21. doi:10.1016/j.desal.2016.10.002.

[8] González D, Amigo J, Suárez F. Membrane distillation: Perspectives for sustainable and improved desalination. Renewable and Sustainable Energy Reviews 2017;80:238–59. doi:10.1016/j.rser.2017.05.078.

[9] Elzahaby AM, Kabeel A, Bassuoni M, Elbar ARA. Direct contact membrane water distillation assisted with solar energy. Energy Conversion and Management 2016;110:397–406. doi:10.1016/j.enconman.2015.12.046.

[10] Fernández-Ibáñez P, Polo-López MI, Malato S, Ruiz-Aguirre A, Zaragoza G. Solar photocatalytic disinfection of water for reuse in irrigation. In: Geothermal, Wind and Solar Energy Applications in Agriculture and Aquaculture. CRC Press; 2017, p. 195–211.

[11] Romero R, Muriel J, García I, de La Peña DM. Research on automatic irrigation control: State of the art and recent results. Agricultural Water Management 2012;114:59–66. doi:10.1016/j.agwat.2012.06.026.

[12] Lozoya C, Mendoza C, Mejía L, Quintana J, Mendoza G, Bustillos M, et al. Model predictive control for closed-loop irrigation. IFAC Proceedings Volumes 2014;47(3):4429–34. doi:10.3182/20140824-6-ZA-1003.02067.

[13] Lozoya C, Mendoza C, Aguilar A, Román A, Castelló R. Sensor-based model driven control strategy for precision irrigation. Journal of Sensors 2016;2016. doi:10.1155/2016/9784071.

[14] Pawlowski A, Sánchez-Molina JA, Guzmán J, Rodríguez F, Dormido S. Evaluation of event-based irrigation system control scheme for tomato crops in greenhouses. Agricultural Water Management 2017;183:16–25. doi:10.1016/j.agwat.2016.08.008.

[15] Roca L, Sánchez-Molina JA, Rodríguez F, Bonilla J, de la Calle A, Berenguel M. Predictive control applied to a solar desalination plant connected to a greenhouse with daily variation of irrigation water demand. Energies 2016;9(3):194. doi:10.3390/en9030194.

[16] Gil JD, Roca L, Ruiz-Aguirre A, Zaragoza G, Berenguel M. Optimal operation of a solar membrane distillation pilot plant via nonlinear model predictive control. Computers & Chemical Engineering 2018;109:151–65. doi:10.1016/j.compchemeng.2017.11.012.

[17] Camacho EF, Berenguel M, Rubio FR, Martínez D. Control of Solar Energy Systems. Springer; 2012.

[18] Camponogara E, Jia D, Krogh BH, Talukdar S. Distributed model predictive control. IEEE Control Systems Magazine 2002;22(1):44–52. doi:10.1109/37.980246.

[19] Rahman M, Oo A. Distributed multi-agent based coordinated power management and control strategy for microgrids with distributed energy resources. Energy Conversion and Management 2017;139:20–32. doi:10.1016/j.enconman.2017.02.021.

[20] Karavas CS, Kyriakarakos G, Arvanitis KG, Papadakis G. A multi-agent decentralized energy management system based on distributed intelligence for the design and control of autonomous polygeneration microgrids. Energy Conversion and Management 2015;103:166–79. doi:10.1016/j.enconman.2015.06.021.

[21] Negenborn RR, van Overloop PJ, Keviczky T, De Schutter B. Distributed model predictive control of irrigation canals. Networks and Heterogeneous Media 2009;4(2):359–80. doi:10.3934/nhm.2009.4.359.

[22] Fele F, Maestre JM, Hashemy SM, de la Peña DM, Camacho EF. Coalitional model predictive control of an irrigation canal. Journal of Process Control 2014;24(4):314–25. doi:10.1016/j.jprocont.2014.02.005.

[23] Farhadi A, Khodabandehlou A. Distributed model predictive control with hierarchical architecture for communication: application in automated irrigation channels. International Journal of Control 2016;89(8):1725–41. doi:10.1080/00207179.2016.1145358.

[24] Scherer HF, Pasamontes M, Guzmán JL, Álvarez J, Camponogara E, Normey-Rico J. Efficient building energy management using distributed model predictive control. Journal of Process Control 2014;24(6):740–9. doi:10.1016/j.jprocont.2013.09.024.

[25] Rubio FR, Navas SJ, Ollero P, Lemos JM, Ortega MG. Control óptimo aplicado a campos de colectores solares distribuidos. Revista Iberoameri-

cana de Automática e Informática industrial 2018;15:327–38. doi:10.4995/riai.2018.8944.

[26] Ruiz-Aguirre A, Andrés-Mañas J, Fernández-Sevilla J, Zaragoza G. Modeling and optimization of a commercial permeate gap spiral wound membrane distillation module for seawater desalination. Desalination 2017;419:160–8. doi:10.1016/j.desal.2017.06.019.

[27] Ruiz-Aguirre A, Andrés-Mañas J, Fernández-Sevilla J, Zaragoza G. Experimental characterization and optimization of multi-channel spiral wound air gap membrane distillation modules for seawater desalination. Separation and Purification Technology 2018;205:212–22. doi:10.1016/j.seppur.2018.05.044.

[28] Zaragoza G, Ruiz-Aguirre A, Guillén-Burrieza E. Efficiency in the use of solar thermal energy of small membrane desalination systems for decentralized water production. Applied Energy 2014;130:491–9. doi:10.1016/j.apenergy.2014.02.024.

[29] Rodríguez F, Berenguel M, Guzmán JL, Ramírez-Arias A. Modeling and control of greenhouse crop growth. Springer; 2015.

[30] Gil JD, Roca L, Zaragoza G, Berenguel M. A feedback control system with reference governor for a solar membrane distillation pilot facility. Renewable Energy 2018;120:536–49. doi:10.1016/j.renene.2017.12.107.

[31] de la Calle A, Roca L, Bonilla J, Palenzuela P. Dynamic modeling and simulation of a double-effect absorption heat pump. International Journal of Refrigeration 2016;72:171–91. doi:10.1016/j.ijrefrig.2016.07.018.

[32] Camacho E, Bordons C. Model Predictive Control. London: Springer-Verlag Ltd; 2004.

[33] Matlab optimization toolbox release 2018a. 2018. The MathWorks, Natick, MA, USA.

[34] Plucenio A, Pagano D, Bruciapaglia A, Normey-Rico J. A practical approach to predictive control for nonlinear processes. IFAC Proceedings Volumes 2007;40(12):210–5. doi:10.3182/20070822-3-ZA-2920.00035.

[35] Becerra AT, Bravo XL. La agricultura intensiva del poniente almeriense. diagnóstico e instrumentos de gestión ambiental. M+ A Revista Electrónica de Medioambiente 2010;(8):18–40.

[36] Sánchez-Molina JA, Rodríguez F, Guzmán JL, Cámara-Zapata JM, Sánchez-Garrido G. Modelado del contenido de agua en el aire interior de un invernadero con sistemas de actuación de humidificación y deshumidficación. In: IX Congresso Ibérico de Agroengenharia. 2017,.